Thermal conductivity of crystalline quartz from classical simulations

Young-Gui Yoon,* Roberto Car, and David J. Srolovitz
Princeton Institute for the Science and Technology of Materials, Princeton University, Princeton, New Jersey 08540, USA

Sandro Scandolo
The Abdus Salam International Center for Theoretical Physics and INFM/Democritos National Simulation Center, I-34014 Trieste, Italy

(Received 10 January 2004; published 19 July 2004)

We calculate the thermal conductivity of crystalline α- and β-quartz in the high-temperature range (500 K to 1100 K) using nonequilibrium molecular dynamics simulations and an empirical interatomic potential. We find that finite-size effects associated with the nonequilibrium dynamics are not negligible, which implies that reliable results for the bulk thermal conductivity of quartz must be obtained by extrapolation to infinite sizes. The calculated thermal conductivity is nearly temperature independent over a wide range of temperature, in agreement with experiment.

DOI: 10.1103/PhysRevB.70.012302 PACS number(s): 66.70.+f, 02.70.Ns, 63.20.−e, 44.10.+i

I. INTRODUCTION

The thermal conductivity of oxide ceramics is important both in the physics of dielectric materials and in technological applications where such materials are used as substrates for microelectronic devices, as thermal barrier coatings, and in the production of refractory materials. Heat conduction in solids can occur either via lattice vibrations, or via electronic excitations, or via radiative processes. Electronic contributions to the thermal conductivity are typically small in insulators, for temperatures much smaller than the excitation gap. Similarly, radiative contributions become important only at very high temperatures, due to the $\sim T^3$ dependence of the radiative term. As a consequence, we restrict our analysis to the lattice contribution. Nonequilibrium molecular dynamics (NEMD) is increasingly employed as a means for calculating the lattice contribution to thermal conductivities, provided an adequate description of atomic bonding in the material of interest is available. This method has been extensively tested and applied to silicon[4,5] and zirconia.[6] Of the oxide ceramics, the silicon oxides are arguably the most technologically important. Therefore, the present study focuses on silicon oxides. Recently, the thermal conductivity of vitreous silica was determined[2] using NEMD and the empirical interatomic potential of van Beest, Kramer, and van Santen (hereafter "BKS").[1] Even though qualitative agreement with experiment was found over a wide temperature range, the calculated thermal conductivity at high temperature ($T > 500$ K) was about a factor of 2 smaller than experiments. The determination of the thermal conductivity of amorphous materials via computer simulations are often complicated by the sensitivity of the structure to the detailed molecular dynamics procedure used to produce the amorphous structure. On the other hand, calculations of thermal conductivity of crystalline materials is unambiguous—independent of the initial configuration provided that the simulation is of sufficient duration to ensure steady-state temperature profiles are established through phonon scattering and provided that the simulation cell is sufficiently large to avoid spurious finite size effects. Finite-size effects are expected to be larger in quartz than in vitreous silica, because phonons in vitreous silica are scattered not only by dynamical disorder, but also by static (topological) disorder, and therefore have a shorter mean free path.

The scope of this paper is to evaluate the capability of NEMD calculations to provide an accurate estimate of the thermal conductivity in crystalline SiO_2. We do so by calculating the lattice contribution to thermal transport along the optical ([0001]) axis of quartz.

The qualitative agreement between our calculations of the thermal conductivity of crystalline quartz with experimental data suggest that thermal conductivity of quartz is dominated by the lattice contribution and that the NEMD can be used to determine thethermal conductivity of crystalline quartz. We also find that the results are affected by important finite-size effects, and that full convergence of the results as a function of the simulation size can be computationally exceptionally demanding. This suggests that the NEMD approach will provide a useful tool for the development of crystalline, SiO_2-based ceramics for thermal conductivity-sensitive applications, but highlights the need for methodological developments capable of reducing the load of the computation.

II. METHOD

The thermal conductivity, κ, is the ratio of the thermal current to the temperature gradient (Fourier's law),

$$\kappa = \frac{J_z}{\partial T/\partial z}, \tag{1}$$

where J_z and $\partial T/\partial z$ are the heat flux per unit area in and the temperature gradient along the z-direction, respectively. The thermal conductivity can be calculated from either nonequilibrium[2,4–15] or equilibrium molecular dynamics[16–21] simulations. We adopt a nonequilibrium molecular dynamics method of velocity rescaling to produce a constant heat flux, as proposed by Jund and Jullien.[2] To calculate the tempera-

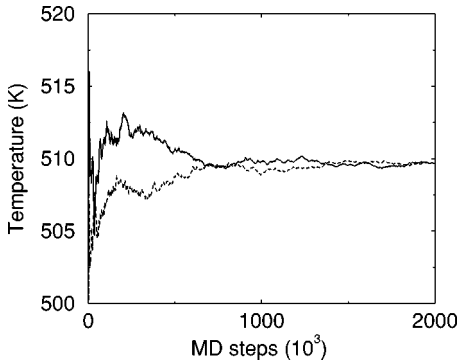

FIG. 1. Two measurements of the time-dependence of the temperature in two slabs, 3.8 nm from the center of the slab where the heat was added.

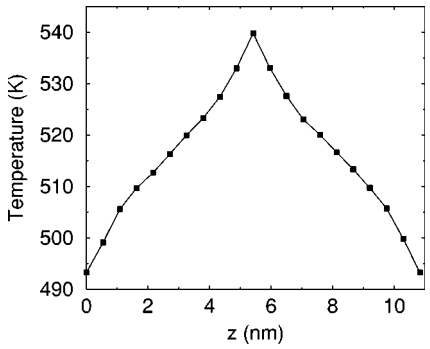

FIG. 2. Typical local temperature profile for temperature gradient calculation.

ture profile, we divide a long simulation cell into a series of thin parallel slabs and measure the temperature in each. Heat is added to the slab at the center of the simulation cell at a fixed rate and removed from a slab at one end of the simulation cell at the same rates by rescaling velocities there at every time step. After sufficient time, this established a temperature profile (gradient) that decreases from the center to the ends of the simulation cell (periodic boundary conditions are enforced). Since a thermal flux is imposed and the temperature gradient is measured, we calculate the thermal conductivity through Eq. (1). In the present calculation, we employ a simulation cell consisting of $4\times4\times20$ hexagonal (9 atom) unit cells (with the long direction parallel to [0001]). The molecular dynamics simulations were performed using a velocity Verlet algorithm with a 0.97 fs time step. We use the popular classical BKS interatomic potential: $\Phi_{ij}=q_iq_j/r_{ij}+A_{ij}e^{-b_{ij}r_{ij}}-C_{ij}/r_{ij}^6$, where r_{ij} is the separation between atoms i and j and the other variables are parameters of the potential which can be found in the original BKS reference.[1] We evaluate the long-range Coulomb terms using the Ewald summation method. The Ewald method is more computationally demanding than other methods based on the truncation of the interaction at finite distances.[6] However, the dynamical properties of silicates are known to be very sensitive to the choice of the potential as well as to the details of the long-range truncation.[22] Therefore, in this work we evaluate Coulomb terms exactly and defer a comparison with truncation methods to a future study.

The time required to establish a steady-state temperature profile varied with temperature from ~12 ns at 1100 K to ~2 ns at 500 K. Following the suggestion of Schelling and Phillpot,[4] we compute the average temperature in each slab through $\langle T(z)\rangle_M=1/M\Sigma_{m=1}^{M-1}T_{N-m}(z)$, where $\langle T(z)\rangle_M$ is the temperature at z averaged over the final M time steps of the simulation, $T_{N-m}(z)$ is the temperature at z in time step $N-m$, and N is the total number of time steps during the entire simulation. A simple measure of the convergence of the measured temperature is the degree to which the temperature in two slabs, equidistant from the slab into which heat is added, agree. The simulation is terminated when this difference is less than 3 K. Figure 1 shows the average temperatures in two slabs, that are equidistant (7 slabs away) from the slab into which heat is added, versus M. This data shows that the average has converged within $M=10^6$ MD steps.

Figure 2 shows a typical time-averaged temperature profile used to compute the thermal conductivity. This data was obtained using a $4\times4\times20$ SiO_2 unit cell simulation cell with a heat flux of 2.97×10^{10} J/m^2 s at 500 K (the heat flux varies slightly with temperature due to the temperature-dependence of the equilibrium lattice parameters). Although the entire temperature profile is nonlinear because of the unphysical manner in which heat is added/removed at the heat source/sink, the profile is very nearly linear over a substantial range between the heat source and sink. Therefore, the temperature gradient is extracted by excluding the 5 slabs around the heat source and 5 slabs around the sink. To further improve the accuracy, we make use of the fact that the system is symmetric about the position of the heat sink. SiO_2 undergoes a phase transition from α-quartz to β-quartz between 800 and 900 K. As a consequence the simulations were performed with the experimentally determined crystal structure (and lattice parameter) at each temperature. Both crystal structures are hexagonal with the same number of atoms per unit cell.

III. FINITE SIZE EFFECTS

Recent simulations[4] demonstrated that the thermal conductivity is nearly independent of the size of the simulation cell in the plane perpendicular to the heat flux. In the same work, however, the thermal conductivity was shown to depend on the length of the simulation cell in the direction of the heat flux. This arises from phonon scattering from the layers where heat is artificially added or removed from the system. Kinetic theory gives the thermal conductivity as

$$\kappa=\tfrac{1}{3}c_v v l, \tag{2}$$

where l is the phonon mean free path, c_v is the constant volume lattice specific heat, and v is the sound velocity. From Eq. (2) the phonon mean free path l is estimated to be $3\kappa/c_v v\approx2$ nm with $c_v\approx3$ J/(cm^3 K), $v\approx6$ km/s, and $\kappa\approx4$ W/(m K). The estimated mean free path and simulation cell sizes are on the same order of magnitude. If the distance between the layers where heat is added or removed $(L_z/2)$ is comparable with the phonon mean free path, then an effective mean free path l_{eff} can be defined as[4]

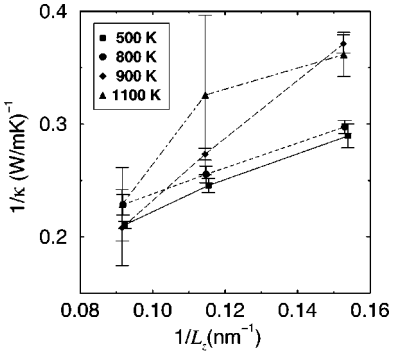

FIG. 3. $1/\kappa$ calculated at four different temperatures is plotted with error bars as $1/L_z$ is changed for different cell sizes.

$$\frac{1}{l_{\text{eff}}} = \frac{1}{l_\infty} + \frac{4}{L_z}. \tag{3}$$

In order to check the effect of finite L_z we carried out simulations using three different cells, with $L_z=\{12,16,20\}c$, respectively, where c is the temperature-dependent lattice parameter along the optical axis [0001]. The lateral size was fixed to 4×4 repeat units of the quartz basal plane. The total number of atoms in the three simulation cells was 1728, 2304, and 2880, respectively. Figure 3 shows the thermal conductivity calculated at four different temperatures with the three cells. At all temperatures the value of $1/\kappa$ decreases for decreasing $1/L_z$, as expected from (3). However, Eq. (3) predicts that $1/\kappa$ should tend linearly with $1/L_z$ to the $L_z \rightarrow\infty$ limit. A linear fit to the data of Fig. 3 has been attempted, but for temperatures above 800 K it provides a vanishing lower limit for $1/\kappa$, which means that we are unable to set an upper limit for κ, based on the present simulations. Such a large uncertainity in the asymptotic value cannot be fully ascribed to statistical errors in the simulations (the error bars in Fig. 3), as in some cases (e.g., at 500 K and 800 K) these errors are quite small. Instead, the uncertainty seems to be connected with the nontrivial dependence of $1/\kappa$ on $1/L_z$. This indicates that finite cell length corrections are significant and that extrapolation of the data to infinite sizes can be more problematic than previously thought. We notice that the values of L_z used in this work are smaller than those reported in Ref. 6 because the choice to avoid truncating the Coulomb tails of the interatomic potentials, as discussed above, results in a considerable increase of the computational load.

IV. RESULTS AND DISCUSSION

Figure 4 shows the thermal conductivity, determined via the simulation method described above, versus temperature. In spite of the large uncertainties, it is interesting to observe that the calculated temperature dependence of κ is rather weak, in accordance with experiments. This is at variance with the typical $1/T^\alpha$ (with $\alpha\gtrsim1$) scaling of the thermal conductivity in crystals at high temperature. Moreover, as already mentioned, SiO_2 transforms from α-quartz to β-quartz between 800 and 900 K, but no major changes are observed in the thermal conductivity.

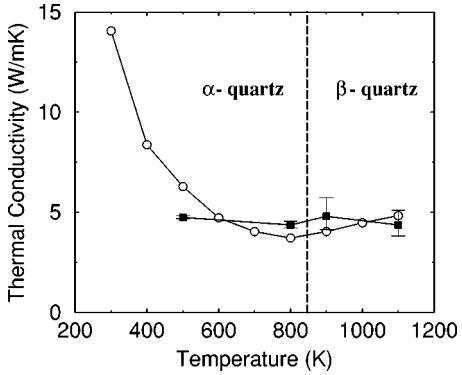

FIG. 4. Comparison of the calculated (filled squares) and experimentally measured (Ref. 3) (open circles) thermal conductivity as a function of temperature. The data at 500 and 800 K were obtained for α-quartz and those at 900 and 1100 K were obtained for β-quartz. The calculated thermal conductivity is plotted with error bars and the experimental transition temperature is 846 K.

Figure 4 also shows the thermal conductivity versus temperature, extracted from experiment. This thermal conductivity was determined from the relation $\kappa=D_T c_p \rho$, where D_T is the thermal diffusivity,[3] c_p is the molar heat capacity,[23] and ρ is the inverse molar specific volume.[24] The computed and experimental thermal conductivities are in qualitative agreement. We notice that the thermal conductivity calculated for amorphous SiO_2 in the same temperature range by Jund and Julien[2] was affected by a similar discrepancy with experiment, but of different sign, their calculated values being about a factor of 2 smaller than experimental values. Their calculation was affected by the uncertainty about the actual structure of amorphous SiO_2. Such an uncertainty is removed here as we consider a crystalline structure. Because we find that BKS yields systematically higher values for κ, it is likely that the atomistic structure of amorphous SiO_2 used in Ref. 2 is not very representative of real glass, a likely consequence of the very fast quenching rate employed to generate it.[25]

Since the calculated thermal conductivity is larger than the measured thermal conductivity, the conclusion that the electronic and radiative contributions to the thermal conductivity are unimportant stands. Of course, the veracity of the prediction depends upon the degree to which the interatomic potential describes the system. After the current paper was submitted, the authors came to know that a relevant paper was published.[26] They calculated thermal conductivity of various silica structures including α-quartz from equilibrium molecular dynamics and obtained a good agreement with experimental data. Thermal conductivity of α-quartz has been decomposed into long range and short range components at 250 K. Therefore, nonequilibrium and equilibrium methods complement each other.

V. CONCLUSION

We have performed the first molecular dynamics simulation to obtain the thermal conductivity of α- and β-quartz using the BKS SiO_2 interatomic potential. The simulations

were performed by imposing a thermal flux and measuring the temperature gradient and extracting the thermal conductivity through Fourier's Law. Just as in the experimental measurements in the $500\ \mathrm{K} \leqslant T \leqslant 1100\ \mathrm{K}$ range, the thermal conductivity was found to be roughly temperature-independent. The observation that the predicted thermal conductivity is greater than in the experiments suggests that electronic and radiative contributions to the thermal conductivity of quartz are relatively unimportant. However, this conclusion rests upon the reliability of the empirical interatomic potential. Large finite-size effects prevent a more accurate determination of the thermal conductivity. However, if finite-size effects scale with the inverse of the length of the simulation box (which is qualitatively, but perhaps not quantitatively true), then the accuracy of a NEMD calculation of thermal conductivity increases linearly with the computational speed. This suggests that NEMD will be an increasingly useful tool to predict the thermal conductivity of ceramics. Future work will then have to focus in more detail on the reliability of interatomic potentials for these systems.

ACKNOWLEDGMENTS

This work was supported by NASA under Grant No. NAG3-2665. Computer time was provided by the W. M. Keck Computational Materials Science Laboratory. S.S. and Y.-G.Y. ackowledge useful discussions with Paul Tangney.

*Current address: Department of Physics, Chung-Ang University, Seoul, Korea.

[1] B. W. H. van Beest, G. J. Kramer, and R. A. van Santen, Phys. Rev. Lett. **64**, 1955 (1990).
[2] P. Jund and R. Jullien, Phys. Rev. B **59**, 13 707 (1999).
[3] H. Kanamori, N. Fujii, and H. Mizutani, J. Geophys. Res. **73**, 595 (1968).
[4] P. K. Schelling, S. R. Phillpot, and P. Keblinski, Phys. Rev. B **65**, 144306 (2002).
[5] A. Maiti, G. D. Mahan, and S. T. Pantelides, Solid State Commun. **102**, 512 (1997).
[6] P. K. Schelling and S. R. Phillpot, J. Am. Ceram. Soc. **84**, 2997 (2001).
[7] C. Oligschleger and J. C. Schon, Phys. Rev. B **59**, 4125 (1999).
[8] A. Baranyai, Phys. Rev. E **54**, 6911 (1996).
[9] R. H. H. Poetzsch and H. Böttger, Phys. Rev. B **50**, 15 757 (1994).
[10] D. J. Evans, Phys. Lett. **91A**, 457 (1982).
[11] M. J. Gillan and M. Dixon, J. Phys. C **16**, 869 (1983).
[12] S. Berber, Y.-K. Kwon, and D. Tomanek, Phys. Rev. Lett. **84**, 4613 (2000).
[13] G. V. Paolini, G. Ciccotti, and C. Massobrio, Phys. Rev. A **34**, 1355 (1986).
[14] F. Müller-Plathe, J. Chem. Phys. **106**, 6082 (1997).
[15] D. Bedrov and G. D. Smith, J. Chem. Phys. **113**, 8080 (2000).
[16] J. Che, T. Cagin, W. Deng, and W. A. Goddard, J. Chem. Phys. **113**, 6888 (2000).
[17] J. Li, L. Porter, and S. Yip, J. Nucl. Mater. **255**, 139 (1998).
[18] S. G. Volz and G. Chen, Phys. Rev. B **61**, 2651 (2000).
[19] Y. H. Lee, R. Biswas, C. M. Soukoulis, C. Z. Wang, C. T. Chan, and K. M. Ho, Phys. Rev. B **43**, 6573 (1991).
[20] A. J. C. Ladd, B Moran, and W. G. Hoover, Phys. Rev. B **34**, 5058 (1986).
[21] R. Vogelsang, C. Hoheisel, and G. Ciccotti, J. Chem. Phys. **86**, 6371 (1987).
[22] J. Horbach and W. Kob, Phys. Rev. B **60**, 3169 (1999).
[23] *CRC Handbook of Chemistry and Physics*, 81st ed. (CRC Press, Boca Raton, 2000).
[24] M. A. Carpenter, E. K. H. Salje, A. Graeme-Barber, B. Wruck, M. T. Dove, and K. S. Knight, Am. Mineral. **83**, 2 (1998).
[25] K. Binder, J. Horbach, and W. Kob, Comput. Sci. Eng. **5**, 60 (2003).
[26] A. J. H. McGaughey and M. Kaviany, Int. J. Heat Mass Transfer **47**, 1799 (2004).